Evolutionary Systematics. 7 2023, 195–209 | DOI 10.3897/evolsyst.7.102950

PENSOFT

EVOLUTIONARY SYSTEMATICS

A third species of glassfrog in the genus *Chimerella* (Anura, Centrolenidae) from central Peru, discovered by an integrative taxonomic approach

Jörn Köhler[1], Pablo J. Venegas[2,3], Ernesto Castillo-Urbina[4], Frank Glaw[5], César Aguilar-Puntriano[4], Miguel Vences[6]

1 *Hessisches Landesmuseum Darmstadt (HLMD), Friedensplatz 1, 64283 Darmstadt, Germany*
2 *Rainforest Partnership, 4005 Guadalupe St., Austin, TX 78751, USA*
3 *Instituto Peruano de Herpetología (IPH), Augusto Salazar Bondy 136, Urb. Higuereta, Surco, Lima, Peru*
4 *Universidad Nacional Mayor de San Marcos, Museo de Historia Natural (MUSM), Departamento de Herpetología, Av. Arenales 1256, Lima 11, Peru*
5 *Zoologische Staatssammlung München (ZSM-SNSB), Münchhausenstr. 21, 81247 München, Germany*
6 *Zoological Institute, Technische Universität Braunschweig, Mendelssohnstr. 4, 38106 Braunschweig, Germany*

https://zoobank.org/FCC50241-B78C-4EDB-8991-B7410EBF186A

Corresponding author: Jörn Köhler (joern.koehler@hlmd.de)

Academic editor: Alexander Haas ♦ **Received** 3 March 2023 ♦ **Accepted** 9 May 2023 ♦ **Published** 16 May 2023

Abstract

We studied the taxonomic status of glassfrogs collected in Departamento Huánuco, central Peru, which in the field were tentatively allocated to *Chimerella*, one of the twelve genera currently recognized in the family Centrolenidae. Detailed analyses of their morphology, bioacoustics, and molecular genetics supported their generic allocation and provided evidence for them representing a divergent and unnamed evolutionary lineage within *Chimerella*. We herein describe this lineage as a new species, being mainly distinguished from the two other known congeners, *C. corleone* and *C. mariaelenae*, by details of colouration in life and preservative, substantial differences in advertisement call, and differentiation in mitochondrial markers (12S rRNA, 16S rRNA, cytochrome *b*) and a nuclear-encoded marker (Rag-1). The new species is the southernmost distributed species in the genus and was found in a swampy habitat at the bank of the Río Patay Rondos, a tributary of the Río Monzon, in rainforest at the Andean-Amazon foothills at 798 m above sea level. Aspects of species delimitation within *Chimerella* and related future research are briefly addressed and discussed.

Key Words

Amphibia, *Chimerella mira*, new species, bioacoustics, molecular genetics, morphology

Introduction

Glassfrogs in the family Centrolenidae, being distributed from Mexico southward to Argentina and southeastern Brazil (Frost 2023), constitute one of the most peculiar groups of Neotropical frogs, not only for their (partly) transparent ventral skin, but also for their complex ecology, behaviour and evolutionary history (e.g., Guayasamin et al. 2008, 2009, 2020; Delia et al. 2017; Taboada et al. 2022). Currently, 163 species of centrolenids are recognized, allocated to twelve genera (Frost 2023). Among these is the genus *Chimerella*, erected by Guayasamin et al. (2009) to accommodate *Centrolene mariaelenae* Cisneros-Heredia and McDiarmid, 2006 from Ecuador, which is phylogenetically sister to all other genera of the tribe Cochranellini. At the time of its description, *Chimerella* was monotypic containing *Chimerella mariaelenae* only. Later, Twomey et al. (2014) described a second species in the genus, *Chimerella corleone*, originating from the Cainarachi valley near Tarapoto (610 m a.s.l.) in the Departamento San Martín, north-eastern Peru.

Knowledge about *Chimerella* glassfrogs remains limited. However, since its description, *C. mariaelenae* has been recorded from northern Peru (Catenazzi and

Venegas 2012) and numerous additional localities in Ecuador (Cisneros-Heredia and Guayasamin 2007; Cisneros-Heredia and McDiarmid 2007; Cisneros-Heredia 2009; Guayasamin et al. 2020). Its larval morphology (Terán-Valdez and Guayasamin 2014) and calls (Batallas and Brito 2016; Guayasamin et al. 2020) have also been described. Knowledge about the second species, *C. corleone*, so far is restricted to information provided in the original species description (Twomey et al. 2014).

During fieldwork in November 2019 in central Peru (see also Castillo-Urbina et al. 2021; Köhler et al. 2022), we collected glassfrogs near the town of Tingo Maria, Departamento Huánuco, among which we tentatively identified two individuals, according to their superficial morphological similarity, as *Chimerella corleone*. However, the subsequent study of the collected specimens, the analysis of molecular markers and call recordings revealed substantial differences to *C. corleone* and provided different lines of evidence for the presence of a third undescribed species in the genus *Chimerella*, which we describe and name herein.

Materials and methods

Fieldwork

Fieldwork was conducted in different areas of north-eastern and central Peru. Specimens were observed and collected during opportunistic searching at night using torchlights and headlamps. Geographic position was recorded using a handheld GPS receiver set to WGS84 datum. Collected specimens were euthanised with an overdose of 5% lidocaine or benzocaine gel applied on the ventral surfaces of individuals (McDiarmid 1994). Tissue samples were taken prior to fixation and stored in 99% ethanol, while specimens were fixed using 96% ethanol or formalin and subsequently stored in 70% ethanol. Specimens were deposited in the herpetological collections of the Museo de Historia Natural, Universidad Nacional Mayor de San Marcos (MUSM), Lima, Peru, and the Centro de Ornitología y Biodiversidad (CORBIDI), Lima, Peru. FGZC refers to Frank Glaw field numbers.

Morphology

Morphometric measurements (in millimetres) were taken by ECU with a digital calliper to the nearest 0.1 mm. For proper comparison, definition of morphological character states, diagnostic and descriptive schemes follow Cisneros-Heredia and McDiarmid (2007) and Guayasamin et al. (2020). Measurements taken and used throughout the text are: SVL, snout–vent length; HL, head length (straight line distance from posterior corner of mouth to the tip of the snout); HW, head width (measured at level of angle of jaws); TD, tympanum diameter (measured horizontally); IND, internarial distance; IOD, interorbital (distance between anterior margins of orbits); ED, horizontal eye diameter; EW, upper eyelid width; END, eye–nostril distance (from anterior margin of orbit to centre of nostril); HaL, hand length (from proximal edge of inner metacarpal tubercle to tip of third finger); TL, tibia length (from the femur-tibia articulation to the tibia-heel proximal articulation); THL, thigh length (from the middle of the cloacal slit to the proximal part of the femur-tibia articulation); FL, foot length (distance from proximal margin of inner metatarsal tubercle to tip of toe IV). Colour in life was described using digital photographs.

Bioacoustics

Vocalizations were recorded using an Olympus LS-5 digital recorder with built-in microphones, at a sampling rate of 44.1 kHz and saved as uncompressed files. Recordings were analysed using the software CoolEdit Pro 2.0 (Syntrillium Software Corp.). Frequency information was obtained through Fast Fourier Transformation (FFT, width 1024 points) with Hanning window function; the audiospectrograms were obtained with Blackman window function at 256 bands resolution. Temporal measurements are given in milliseconds (ms) or seconds (s), as range, with mean ± standard deviation in parentheses. Analysis of calls and terminology in call descriptions follows the recommendations of Köhler et al. (2017), using the note-centered terminological scheme. The recording is provided at the Zenodo repository (https://doi.org/10.5281/zenodo.7896188).

Molecular genetics

Our genetic analyses aimed at identifying divergence among lineages of *Chimerella*. In addition to *Chimerella* samples obtained by our own fieldwork, we searched for available GenBank sequences of *Chimerella*, and also included a limited set of sequences representing all genera currently recognized in the family Centrolenidae for a representative taxon sampling. *Allophryne ruthveni*, family Allophrynidae, the sister taxon of Centrolenidae (Guayasamin et al. 2009), was chosen as the outgroup.

To reconstruct the phylogenetic relationships among *Chimerella* samples, we combined sequences of three mitochondrial genes: one fragment of the 12S rRNA gene (12S), two fragments of the 16S rRNA gene (16S), and one fragment of the cytochrome *b* gene (cob). We extracted DNA from tissue samples using a standard salt protocol and PCR-amplified the gene fragments with the following primers: 12SAL (AAACTGGGATTAGATACCCCACTAT) and 16SR3 (TTTCATCTTTCCCTTGCGGTAC) of Kocher et al. (1989) and Hrbek and Larson (1999) with PCR protocol 94 °C (90 s), [94 °C (45 s), 52 °C (45 s), 72 °C (90 s) × 33], 72 °C (300 s); 16SL3 (AGCAAAGAHYWWACCTCGTACCTTTTGCAT) and 16SAH (ATGTTTTTGATAAACAGGCG) of Vences et al. (2003) with PCR protocol 94 °C (90 s), [94 °C (45 s), 52 °C (45 s), 72 °C (90 s) × 33], 72 °C (300 s); 16SAr-L (5'–CGCCTGTTTATCAAAAACAT–3') and 16SBr-H (5'–CCGGTCTGAACTCAGATCACGT–3')

of Palumbi et al. (1991) with PCR protocol: 94 °C (90 s), [94 °C (45 s), 50–53 °C (45 s), 72 °C (90 s) × 36–40], 72 °C (300 s); and Cytb-a (CCATGAGGACAAATATCATTYTGRGG) and Cytb-c (CTACTGGTTGTCCTCCGATTCATGT) of Bossuyt and Milinkovitch (2000) with PCR protocol 94 °C (90 s), [94 °C (30 s), 53 °C (45 s), 72 °C (90 s) × 35], 72 °C (600 s). Furthermore, we sequenced fragments of a single-copy protein-coding nuclear-encoded gene, the recombination-activating gene 1 (Rag-1) with a nested PCR approach, first using the primers Rag1-Mart Fl1 (AGCTGGAGYCARTAYCAYAARATG) and Rag-1Mart R6 (GTGTAGAGCCARTGRTGYTT), modified from Martin (1999), and then Rag-1AmpF2 (ACNGGNMGICARATCTTYCARCC) and Rag-1-UC-R TTGGACTGCCTGGCATTCAT of Chiari et al. (2004), with PCR protocol 94 °C (240 s), [94 °C (45 s), 45 °C (40 s), 72 °C (120 s) × 45], 72 °C (600 s) for both PCR rounds.

PCR products were purified with Exonuclease I and Shrimp Alkaline Phosphatase digestion, and the purified products along with sequencing primers were shipped to LGC Genomics (Berlin) for sequencing on automated capillary sequencing instruments. Chromatograms were checked for base-calling errors and edited with CodonCode Aligner 6.0.2 (Codon Code Corporation, Dedham, MA, USA). Newly generated sequences were submitted to GenBank (accession numbers OQ877056–OQ877069, OQ888203–OQ888210, and OQ888212–OQ888219). A table with all samples used, the associated GenBank accession numbers and sequences, as well as voucher number and locality, is available from the Zenodo repository (https://doi.org/10.5281/zenodo.7896188) along with the alignment files.

Sequences of the focal *Chimerella* samples were combined with sequences obtained from GenBank. For the cob gene, very few comparative sequences were available and the dataset therefore mostly consists of sequences obtained in our own study for samples of *Chimerella*. The combined sequences of the mitochondrial genes for 12S, 16S (two fragments), and cob were aligned with MAFFT (Katoh and Standley 2013) as implemented in Concatenator (Vences et al. 2022). We then used Concatenator to assemble a combined alignment partitioned by gene, and analysed it in IQ-Tree 1.6.12 (Nguyen et al. 2015). We used Modelfinder (Kalyaanamoorthy et al. 2017) in IQ-Tree with the MFP+MERGE setting to determine the best partition and substitution models and subsequently ran tree inference under the maximum likelihood optimality criterion, with 1000 standard bootstrap replicates to test robustness of nodes. Based on the Modelfinder results, the analysis was run with a partition of two character subsets: (i) 12S and the two 16S fragments, with a TIM2+F+I+G4 model; and (ii) cob, with a TIM2+F+G4 model. We furthermore performed unpartitioned ML analyses of the same data set with MEGA7 (Kumar et al. 2016) under a GTR+G substitution model selected by the Bayesian Information Criterion in MEGA. To quantify genetic divergences, we calculated uncorrected pairwise distances among the 16S sequences (p-distances) in MEGA7.

The alignment of the nuclear Rag-1 gene was analysed separately from the mitochondrial sequences, with the goal to assess concordance in the differentiation of a nuclear encoded and a mitochondrial gene. Sequences of Rag-1 were aligned with the Muscle alignment option, and the nuclear gene alignments trimmed in MEGA7 (Kumar et al. 2016). We then graphically visualized relationships among alleles (haplotypes) of Rag-1 using a haplotype network approach. Alleles (haplotypes) of the nuclear gene were inferred using the PHASE algorithm (Stephens et al. 2001) implemented in DnaSP (Version 5.10.3; Librado and Rozas 2009), a Maximum Likelihood tree from the phased sequences inferred under the Jukes-Cantor substitution model in MEGA7, and this tree used along with the respective alignment as input for Haploviewer (written by G. B. Ewing; http://www.cibiv.at/~greg/haploviewer), a software that implements the methodological approach of Salzburger et al. (2011).

For a formal species delimitation analysis, we used ASAP (Puillandre et al. 2021) as implemented in iTaxoTools (Vences et al. 2021) on a trimmed alignment (475 bp) of the 16S 3' fragment, which was available from all *Chimerella* individuals.

Nomenclatural act

The electronic version of this article in Portable Document Format (PDF) will represent a published work according to the International Commission on Zoological Nomenclature (ICZ), and hence the new name contained in the electronic version is effectively published under that Code from the electronic edition alone. This published work and the nomenclatural acts it contains have been registered in ZooBank, the online registration system for the ICZN. The ZooBank LSIDs (Life Science Identifiers) can be resolved and the associated information viewed through any standard web browser by appending the LSID to the prefix http://zoobank.org/. The LSID for this publication is: https://zoobank.org/FCC50241-B78C-4EDB-8991-B7410EBF186A.

Results

Molecular relationships

Our Maximum Likelihood tree (Fig. 1), based on 2326 nucleotides of the combined mitochondrial DNA sequences (12S and 16S rRNA and cob), grouped with high support species into genera according to current centrolenid classification and recovered the two subfamilies Centroleninae and Hyalinobatrachinae. However, many deep nodes in the tree were poorly supported (bootstrap proportions often <50%), indicating that the combined gene fragments contained insufficient phylogenetic information to reliably resolve intergeneric relationships within the Centrolenidae. Our tree contains a polytomy with respect to the genus *Ikakogi* and the subfamily Hyalinobatrachinae, which is unsurprising

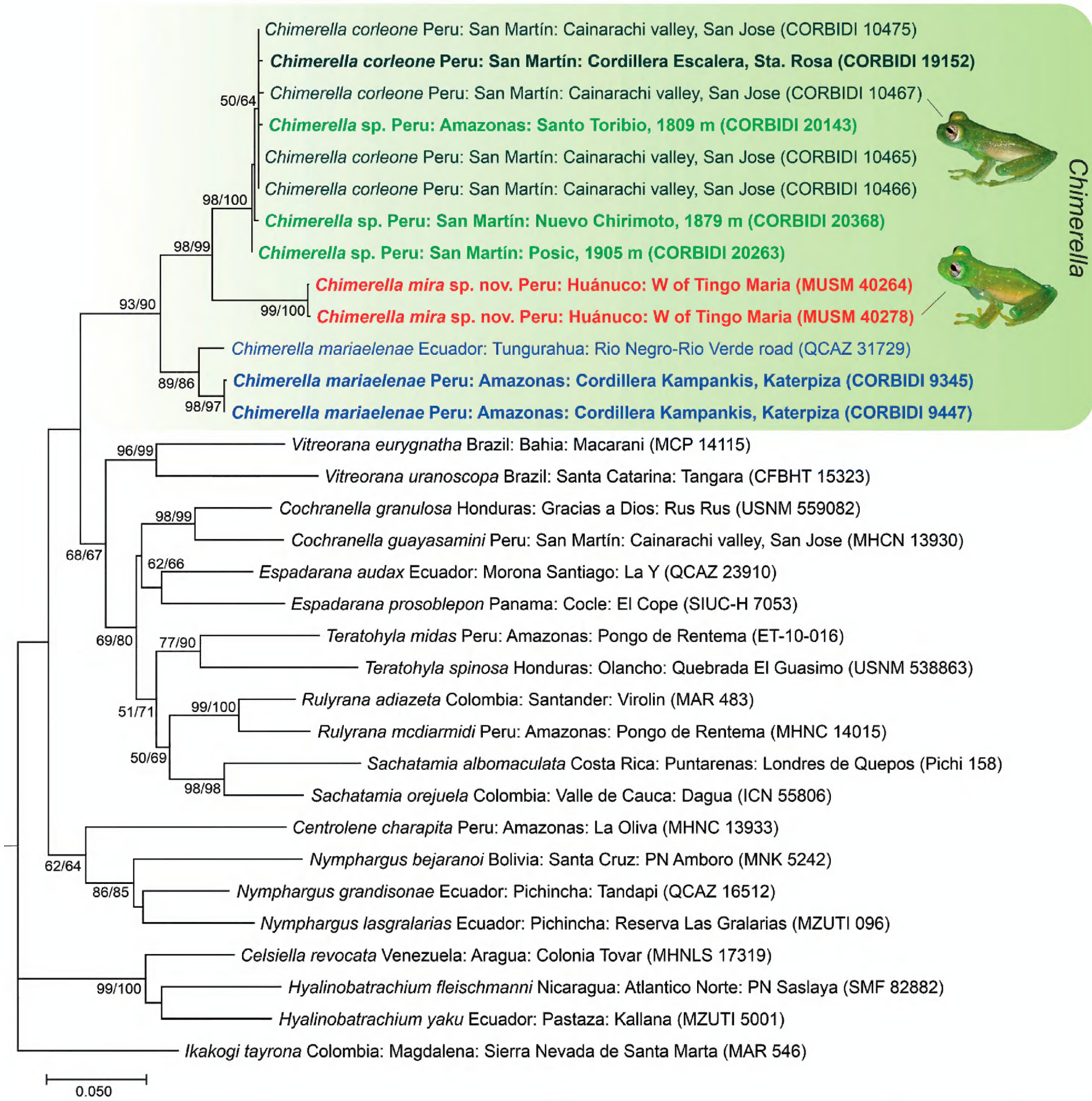

Figure 1. Maximum Likelihood phylogenetic tree of centrolenid frogs inferred from an alignment of 2326 nucleotides of the mitochondrial genes 12S and 16S rRNA, and cytochrome *b*. *Allophryne ruthveni* was used to root the tree (removed for better graphical presentation). Numbers at nodes are bootstrap values in percent calculated with MEGA (500 replicates; not shown if <50%) and IQ-Tree (1000 replicates; not shown if <50). Sequences from samples in bold font were newly obtained for this study. The taxon name is followed by the sample locality and number of the voucher specimen (as provided in GenBank) in parentheses. Inset photos depict the holotypes in life of *Chimerella corleone* (CORBIDI 10467) and *C. mira* sp. nov. (MUSM 40278), respectively.

given that more comprehensive phylogenetic studies revealed the uncertain relationships of *Ikakogi* within Centrolenidae (see Guayasamin et al. 2009; Hutter et al. 2013a).

With regard to the focal genus *Chimerella*, the newly collected central Peruvian samples from west of Tingo Maria form a highly supported clade being sister to *C. corleone* from the type locality and nearby sites in the Cainarachi valley, plus three samples from higher elevations in the Departamentos Amazonas and San Martín. We tentatively refer to these high-elevation samples as *Chimerella* sp. and not *C. corleone*, as they differ remarkably in morphology and need further research. The clade containing *C. corleone*, *C.* sp. and the new samples from central Peru is sister to *C. mariaelenae*. In summary, our analysis reveals three distinct and highly supported clades within the genus *Chimerella*, one representing *C. corleone* (including high elevation populations in need of taxonomic clarification), one representing *C. mariaelenae*, and a third containing our samples from central Peru. Furthermore, among the limited samples available from these three *Chimerella* clades, no haplotype sharing was detected in the nuclear-encoded Rag-1 gene fragment (1021 nucleotides; Fig. 2).

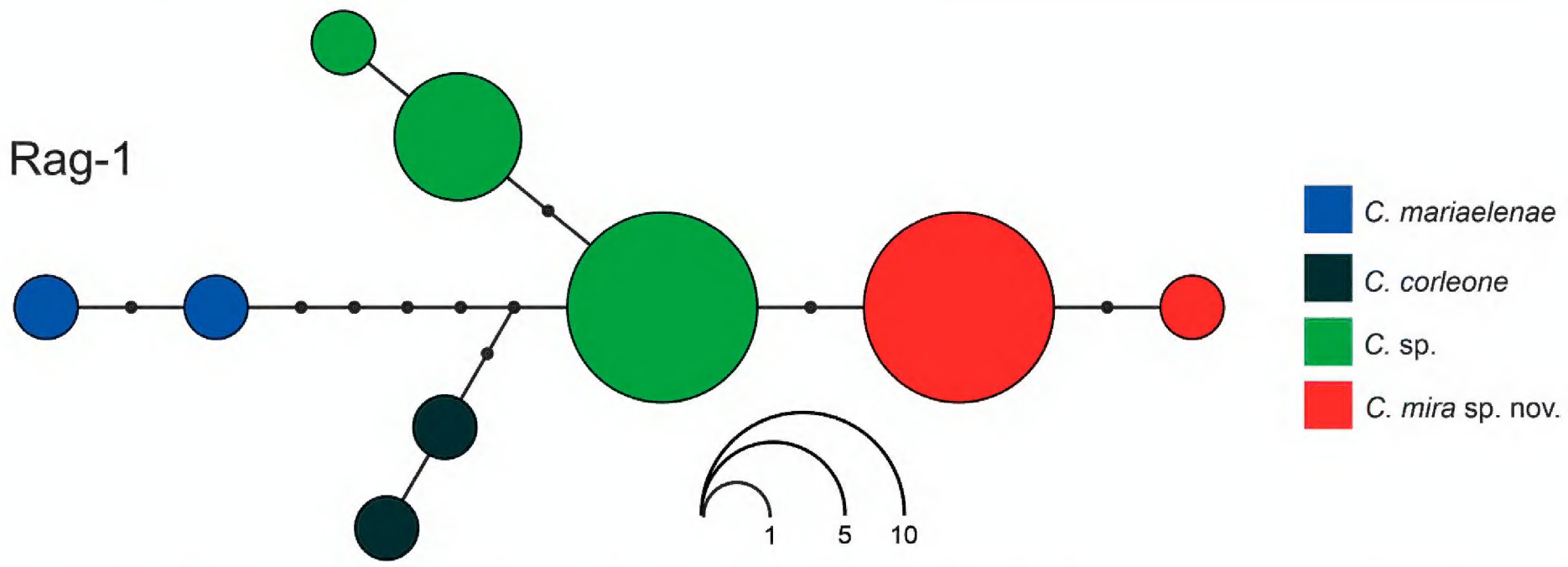

Figure 2. Haplotype network based on 1021 nucleotides of the nuclear-encoded Rag-1 gene from seven specimens of *Chimerella* (based on phased alleles, each specimen is therefore represented twice in the network). Size of circles represents number of times the allele was observed. Colours chosen correspond to those of mitochondrial lineages in Fig. 1.

Uncorrected p-distances in the 16S rRNA gene (for a fragment of 523 nucleotides at the 3' terminus of the gene) among studied samples of *Chimerella* are as follows: Between the new species and *C. corleone*, p-distances range from 3.6–4.0%; between the new species and *C. mariaelenae* they range from 3.5–3.8%; between *C. corleone* and *C. mariaelenae* they range from 3.7–4.0%; between the new species and *Chimerella* sp. they range from 3.2–3.8%; between *C. mariaelenae* and *C.* sp. they range from 3.3–3.8%; and between *C. corleone* and *C.* sp. they range from 0.2–0.6%. Apart from the low genetic divergence observed between *C. corleone* and *C.* sp., distances are in a similar or higher range when compared to distances of congeneric species pairs of other centrolenids, as revealed by cross-checking available GenBank sequences.

The best species partition suggested by ASAP, with a score of 1.5, supported the presence of three subsets in the 16S data, corresponding to (a) *C. corleone* plus the three specimens from Nuevo Chirimoto, Posic, and Santo Toribio, (b) *C. mariaelenae*, and (c) the focal specimens from central Peru (graphic presentation of result available from the Zenodo repository, DOI: 10.5281/zenodo.7896188).

Morphology

Our examination of morphological character states of newly collected specimens and their comparison with described species of *Chimerella* revealed shared character states confirming their allocation to *Chimerella* (humeral spine in males, transparent ventral parietal peritoneum, white pericardial, hepatic and visceral peritonea; see Guayasamin et al. 2009). However, details of dorsal colouration in life, iris colouration, colour in preservative and snout shape revealed a few constant qualitative differences among the mitochondrial clades identified, providing further indication of these representing divergent evolutionary lineages.

Bioacoustics

Although call recordings are sparse, our analysis of recordings and published call descriptions (see below) revealed qualitative and quantitative differences among the calls of individuals assigned to the three mitochondrial clades. Calls of *C. corleone* and *C. mariaelenae* differ from those of the population from central Peru by containing simple single pulse 'Tic' notes versus multi-pulsed 'Trii' notes (sensu Duarte-Marín et al. 2022). Moreover, note duration in calls of *C. corleone* and *C. mariaelenae* is much shorter (4–7 and 10–15 ms, respectively) when compared to calls of the central Peruvian population (42–85 ms). These findings constitute a very strong indication of respective lineage divergence, as the differences observed are far beyond those to be expected from intra-specific call variation (see Köhler et al. 2017), particularly in centrolenids which commonly exhibit rather similar calls among different species (e.g., Guayasamin et al. 2020; Duarte-Marín et al. 2022).

In summary, our results from the analyses of molecular genetics, morphology and bioacoustics provide independent lines of evidence for the central Peruvian samples of *Chimerella* representing a distinct divergent evolutionary lineage which so far remains undescribed and is herein named:

***Chimerella mira* sp. nov.**

https://zoobank.org/3CAA6F1E-9AE5-43FD-8CC5-7CDBEAD44A8B

Type material. ***Holotype.*** MUSM 40278 (FGZC 6233), adult male (Fig. 3a–c), from a point approximately 16 km airline west of Tingo Maria (09°18.09'S, 76°08.71'W, 798 m above sea level), close to the settlement "Corvina Colorada", at the bank of the Río Patay Rondos, Provincia Leoncio Prado, Departamento Huánuco, Peru, collected on 6 November 2019 by Ernesto Castillo-Urbina, Frank Glaw and Jörn Köhler.

Paratype. MUSM 40264 (FGZC 6215), adult male (Fig. 3), same data as holotype, but collected on 5 November 2019.

Etymology. The specific epithet is a Latin adjective (feminine form) meaning 'surprising'. It refers to the fact that this species surprisingly turned out to be undescribed, after at first impression in the field having been tentatively identified as *C. corleone*.

Definition. A species in the genus *Chimerella*, based on molecular relationships and shared morphological traits, characterized by the following combination of characters: (1) dentigerous processes of vomer and vomerine teeth absent; (2) snout truncate in dorsal view, truncate in lateral profile; canthus rostralis straight in dorsal view, rounded in cross-section; nostrils flush with surrounding skin; (3) tympanum and tympanic annulus evident, round, its diameter about 25% of eye diameter; supratympanic fold weakly defined, not concealing upper tympanum; (4) dorsal skin finely shagreened, with few minute scattered dorsal tubercles; skin on venter and ventral surfaces of thighs granular; (5) a pair of enlarged subcloacal warts; (6) ventral parietal peritoneum transparent (condition P0 sensu Cisneros-Heredia and McDiarmid 2007); iridophores in pericardium and peritonea covering digestive tract; kidneys and urinary bladder lacking iridophores (condition V5); (7) liver with two broadly rounded right/left lobes, not forming free flaps, covered by iridophores (condition H1); (8) humeral spine and single subgular vocal sac present in adult males; (9) webbing absent between fingers I and II, basal webbing between fingers II and III; webbing formula $II2^{-}$–$3^{-}III2^{+}$–$2^{+}IV$; (10) webbing between toes extensive; webbing formula $I1^{+}$–$2^{+}II1^{+}$–$2.5III1^{+}$–$3^{-}IV3^{-}$–$1^{+}V$; (11) enamelled fringe present on postaxial edge of finger IV; ulnar fold diffuse; tarsal fold absent; enlarged tubercles on ventrolateral edges of arm and tarsus absent; (12) concealed prepollex, not enlarged, prepollical spine not projecting; nuptial pad absent, but diffuse nuptial excrescence formed by glandular clusters (Type V); (13) finger I slightly longer than finger II; (14) diameter of eye three times wider than width of disc on finger III; (15) in life, dorsum yellow-green with small round scattered pale-yellowish flecks; venter transparent white; bones green; (16) in preservative, dorsum lavender with small scattered round cream flecks; dorsal surfaces of limbs yellowish cream, with scattered melanophores; ventral surfaces yellowish cream; (17) in life, iris silvery white with fine black spotting, and a dark brown median streak formed by fine spots; circumpupillary ring absent; (18) dorsal surfaces of fingers and toes lacking melanophores, except for toes IV and V; (19) males call from the upper surface of leaves; calls consist of 2–3 high-pitched pulsed notes ('Trii' calls sensu Duarte-Marín et al. 2022), 42–85 ms note duration, 160–239 ms inter-note interval duration within calls; dominant frequency 5543–6135 Hz; (20) fighting behavior unknown (but probably present in males; see below); (21) egg clutches unknown; (22) tadpoles unknown; (23) minute body size (sensu Guayasamin et al. 2020), SVL in adult males 18.1–19.6 mm (n = 2); females unknown.

Diagnosis. The new species is morphologically most similar to *C. corleone*. However, it differs from *C. corleone* by fine dark spots in the iris in life (versus dark reticulation; Figs 4, 5), a truncate snout in lateral profile (versus slightly rounded; Fig. 6), tarsal fold absent (versus present as a line of low white warts on the lateral edge of tarsus), greyish-lavender dorsal colour in preservative (versus greyish-green), a dispersed network of melanophores on dorsal surfaces resulting in a light yellow-green colour in life (versus a very dense network of melanophores on dorsal surfaces, resulting in dark green life colouration; Figs 3, 4), a call consisting of pulsed 'Trii' notes (sensu Duarte-Marín et al. 2022) with 42–85 ms duration (versus simple 'Tic' notes of 10–15 ms duration), and substantial differentiation in certain molecular markers. The new species mainly differs from *C. mariaelenae* by a yellow-green dorsum with small round scattered yellowish flecks (versus green dorsum with black flecks and punctuation; Fig. 7), greyish-lavender dorsum with small round cream flecks in preservative (versus pale lavender with dark lavender flecks), silvery white iris in life (versus orange to reddish iris), an advertisement call consisting of pulsed 'Trii' notes with 42–85 ms duration (versus simple 'Tic' notes of 4–7 ms duration; Guayasamin et al. 2020), and substantial differentiation in certain molecular markers.

Description of the holotype. Adult male, SVL 19.6 mm, in good state of preservation (Fig. 8). HW about 1/5 wider than body; HW 29% of SVL; HW 1.15 times HL. Snout truncate in dorsal view, truncate in lateral profile (Fig. 6a); END/ED 0.65; END/IOD 0.55. Loreal region concave, nostrils flush with surrounding skin, round; internarial region concave anterodorsally; canthus rostralis well defined, straight in dorsal view, rounded in cross-section. Eyes directed anterolaterally, angled 51° relative to midline of body (where anteriorly facing eyes would be 90° relative to midline); ED 3.0 times wider than width of disc on finger III; ED 41% of HL and 100% of IOD. Tympanum noticeable with tympanic annulus visible, more evidently ventrally than dorsally, annulus and membrane coloured as dorsum; supratympanic fold weakly defined leaving entire tympanum visible, tympanum round with slight dorsal inclination. Dentigerous processes on vomers absent; dentigerous process on premaxillae and maxillae present; choanae large, circular, separated more widely than nostrils; tongue removed for tissue sample; vocal slits present, wide, oblique and lateral to the tongue. Forelimbs moderately robust, with forearm flattened and roughly 1.4 times as wide as arm; ulnar fold present, low diffuse, white; tubercles on ventrolateral edge of arm absent; humeral spine externally visible as an elongated bump, slightly less defined in preservative than in life. Relative length of fingers: II < I < IV < III; finger discs distinctly expanded, those on fingers I and II rounded, on fingers III and IV slightly truncate, larger than toe discs;

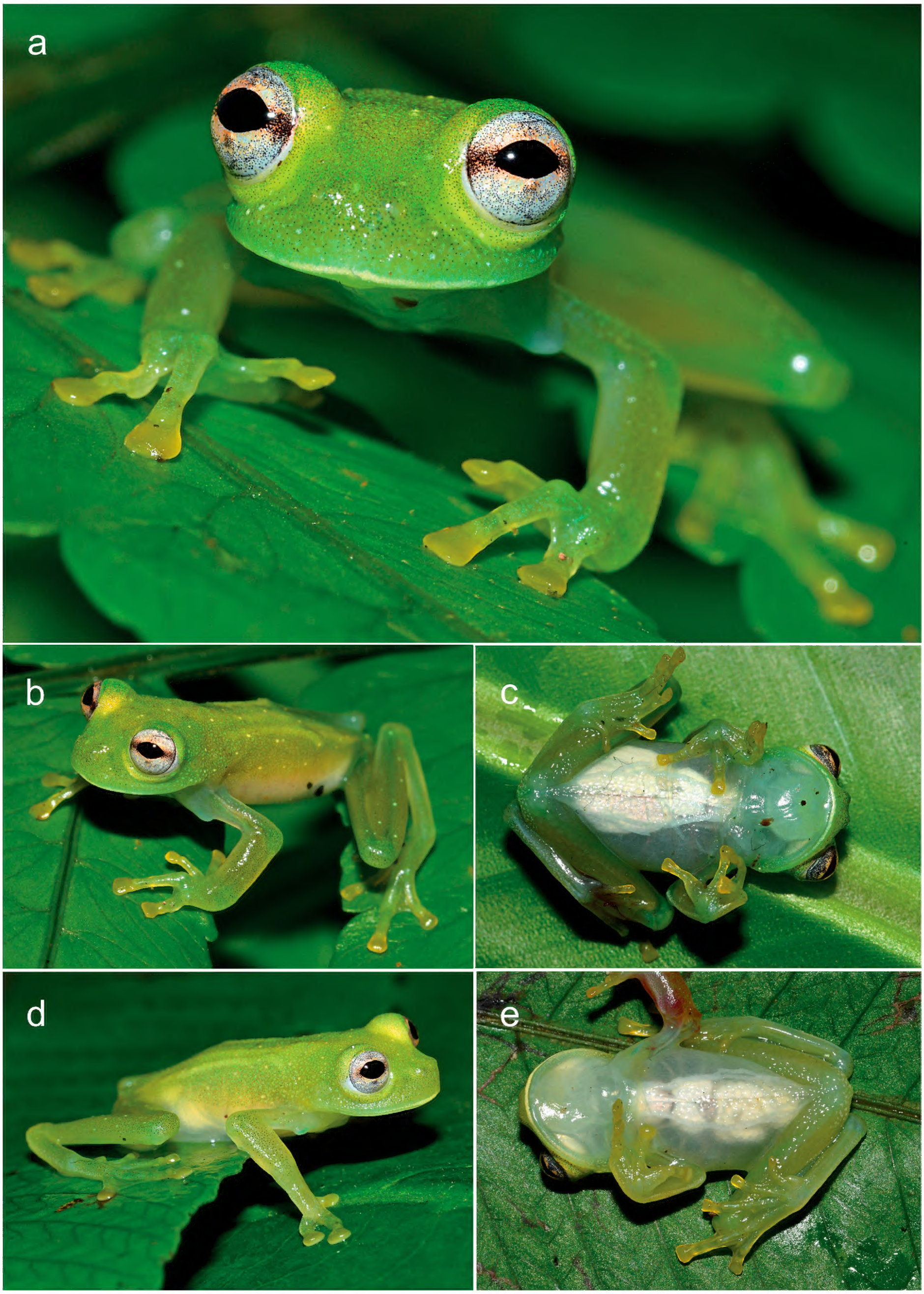

Figure 3. *Chimerella mira* sp. nov. from west of Tingo Maria in life: male holotype (MUSM 40278, FGZC 6233) in **a** frontal, **b** dorsolateral, and **c** ventral views; male paratype (MUSM 40264, FGZC 6215) in **d** lateral and **e** ventral views.

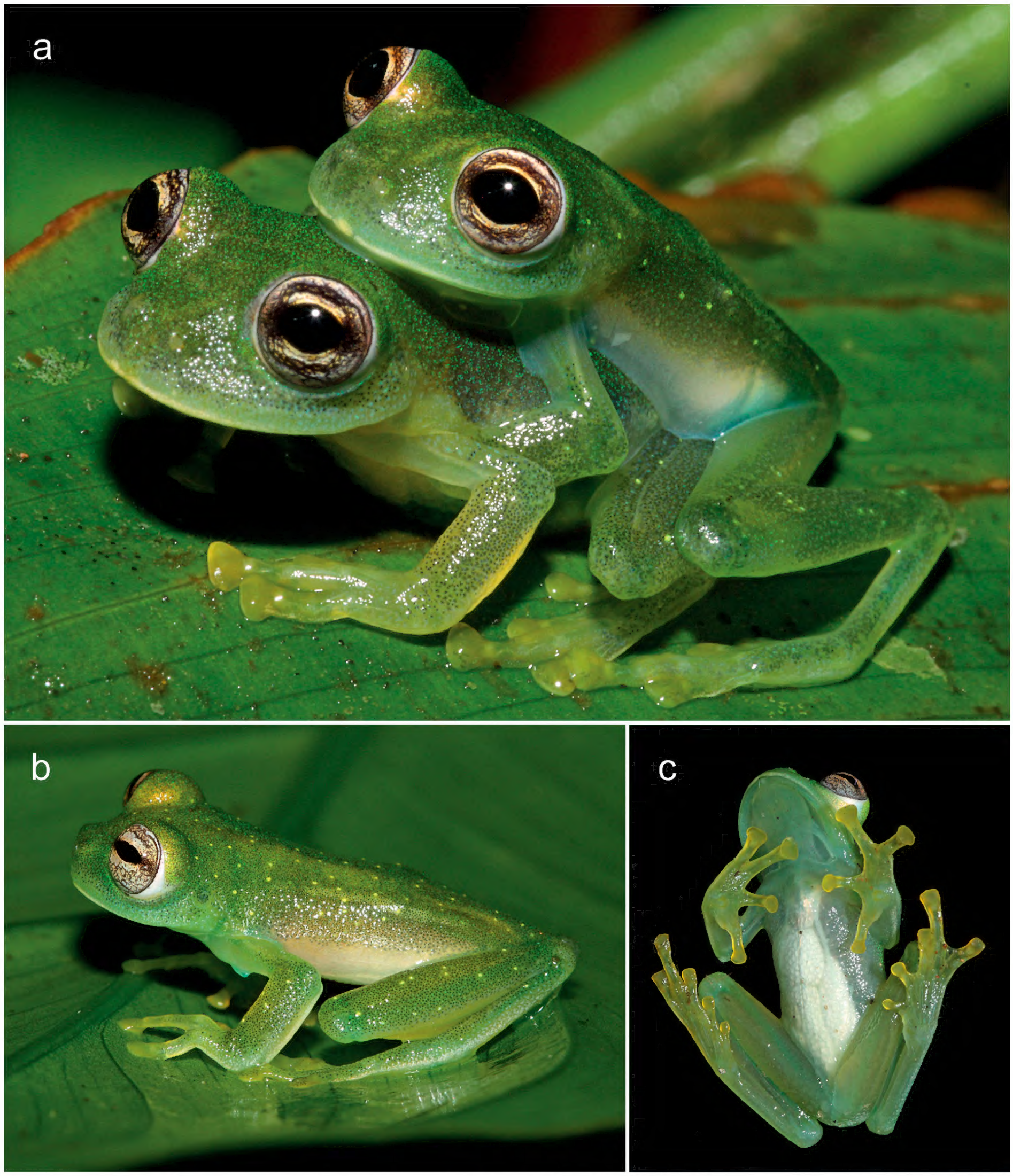

Figure 4. *Chimerella corleone* in life: **a** dorsolateral view of amplectant couple from the type locality photographed at night (note the striking dark reticulation of the iris); **b** dorsolateral and **c** ventral views of the male holotype (CORBIDI 10467). Courtesy of J. Delia and E. Twomey.

width of disc on finger III 32% of ED; webbing absent between fingers I and II, basal webbing between fingers II and III, webbing formula II2^{-}–3^{-}III2^{+}–2^{+}IV. Prepollex concealed; subarticular tubercles round, evident; supernumerary tubercles absent, palmar tubercle round and small, thenar tubercle barely distinct, minute, ovoid; nuptial pads absent, but diffuse nuptial excrescence formed by glandular clusters (Type V sensu Guayasamin et al. 2020). Hind limbs slender, TL 51% of SVL; tarsal fold absent; tubercles on ventrolateral edge of tarsus absent. Relative length of toes: I < II < III < V < IV; toe discs slightly expanded, round; inner metatarsal tubercle narrow, elongated, ovoid, slightly protruding; outer metatarsal tubercle not visible. Webbing formula of feet: I1^{+}–2^{+}II1^{+}–2.5III1^{+}–3^{-}IV3^{-}–1^{+}V. Dorsal skin finely shagreened, with few small scattered cream coloured tubercles on dorsum and dorsal surfaces

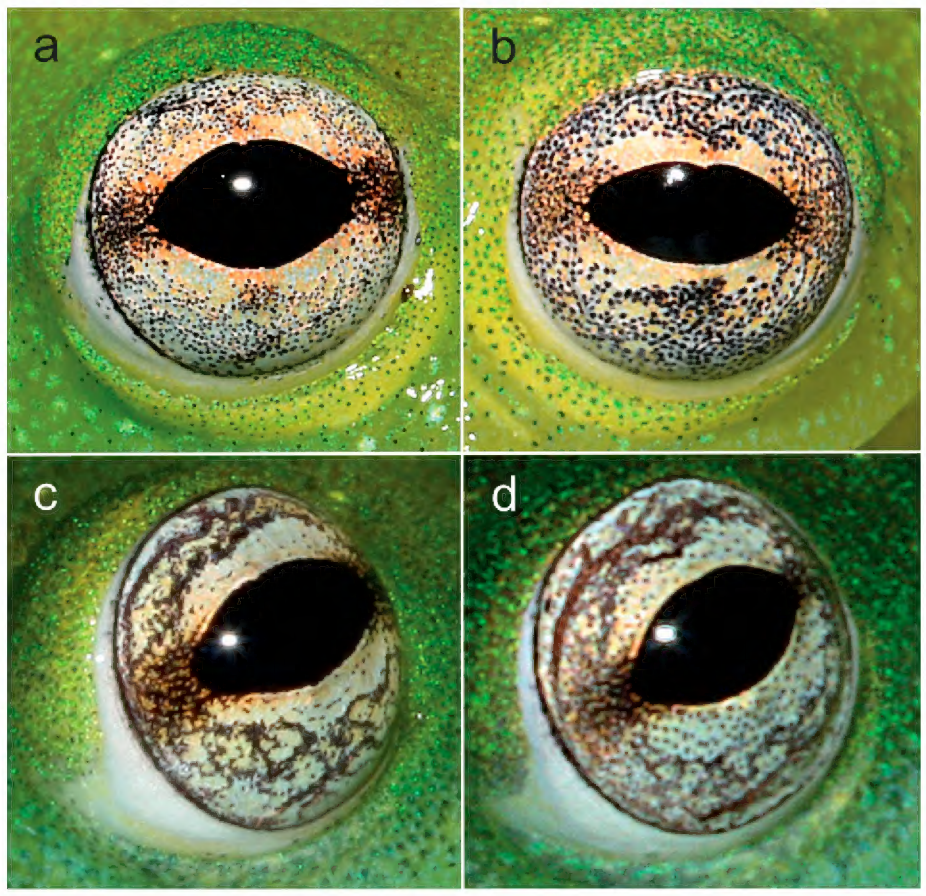

Figure 5. Comparison of eye colouration in life: **a** male holotype (MUSM 40278) and **b** male paratype (MUSM 40264) of *Chimerella mira* sp. nov.; **c** male holotype (CORBIDI 10467) and **d** female paratype (CORBIDI 10465) of *Chimerella corleone* (courtesy of J. Delia and E. Twomey). Note the fine dark spotting versus dark reticulation in the iris.

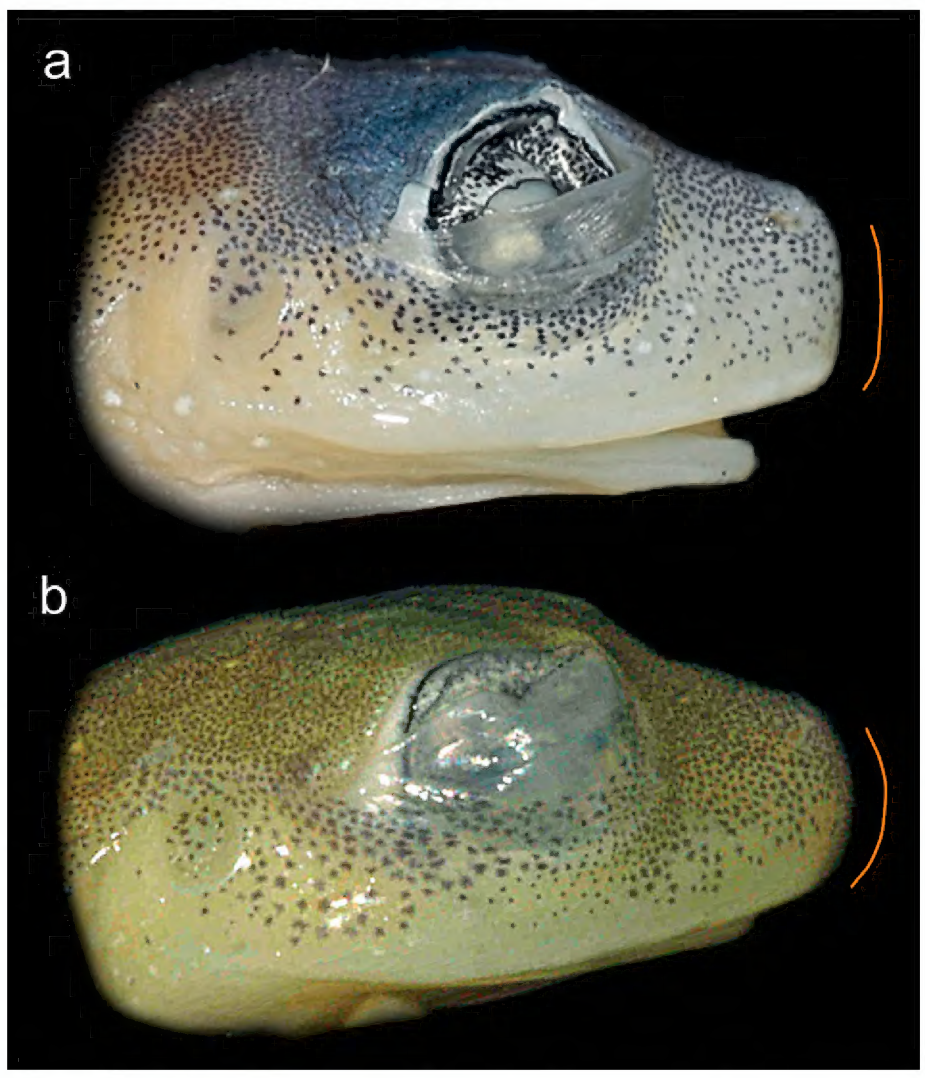

Figure 6. Lateral views of heads of preserved holotypes of **a** *Chimerella mira* sp. nov. (MUSM 40278) and **b** *Chimerella corleone* (CORBIDI 10467; courtesy of E. Twomey). Orange lines indicate outline of snout shape in lateral profile. Not to scale.

of limbs; skin on venter and ventral sides of thighs granular, skin on throat smooth; cloacal opening at level of upper thighs, concealed by faint superior dermal fold; a pair of round, low, unpigmented subcloacal warts present on ventral side; crenulated flaps absent.

Figure 7. Amplectant couple of *Chimerella mariaelenae* from the Cordillera de Kampankis, 1100 m a.s.l., Departamento Amazonas, Peru, in life.

Measurements (in mm). SVL 19.6, HL 5.8, HW 6.7, TD 0.7, IND 1.5, IOD 2.7, ED 2.7, EW 1.2, END 1.5, HaL 5.4, TL 9.9, THL 10.8, FL 7.9.

In life (Fig. 3), dorsal surfaces translucent yellow-green, with small, round, widely scattered yellowish cream flecks on dorsum and dorsal surfaces of thighs; dorsal surfaces of hands and feet yellow-green; dorsal surfaces of finger and toe discs orange-yellow; area around nostrils, dorsal surfaces of arms and thighs dusted with minute dark melanophores; upper lip with a narrow tan line anteriorly that vanishes posteriorly; venter transparent, whitish; throat transparent with a turquoise tint; ventral surfaces of limbs lemon green; ventral surfaces of finger and toe discs orange-yellow; greyish-white diffuse line along lateral edge of proximal ulna; diffuse white spots in cloacal area; subcloacal wart ornamentation transparent; parietal peritoneum transparent; pericardium, hepatic peritonea and visceral peritonea white, urinary bladder transparent; iris silvery white with fine black spotting, median brown streak formed by densely spaced fine spots, circumpupillary ring absent, posterior iris periphery white.

After three years in preservative, dorsum greyish-lavender with scattered small cream flecks; dorsal surfaces of limbs yellowish cream with minute scattered melanophores; dorsal surfaces of hand and fingers yellowish cream; dorsal surfaces of feet and toes yellowish cream, with scattered melanophores extending on dorsal surfaces of toes IV and V; posterior surfaces of thighs yellowish cream; venter and ventral surfaces of arms and legs yellowish cream, throat cream (Fig. 8).

Variation. Overall, the male paratype MUSM 40264 is rather similar to the holotype. In life, it had a slightly paler green dorsal colouration, with fewer and less distinct minute yellowish flecks on dorsum. The throat lacked the turquoise tint and the brown median streak in the iris was less distinctly expressed when compared to

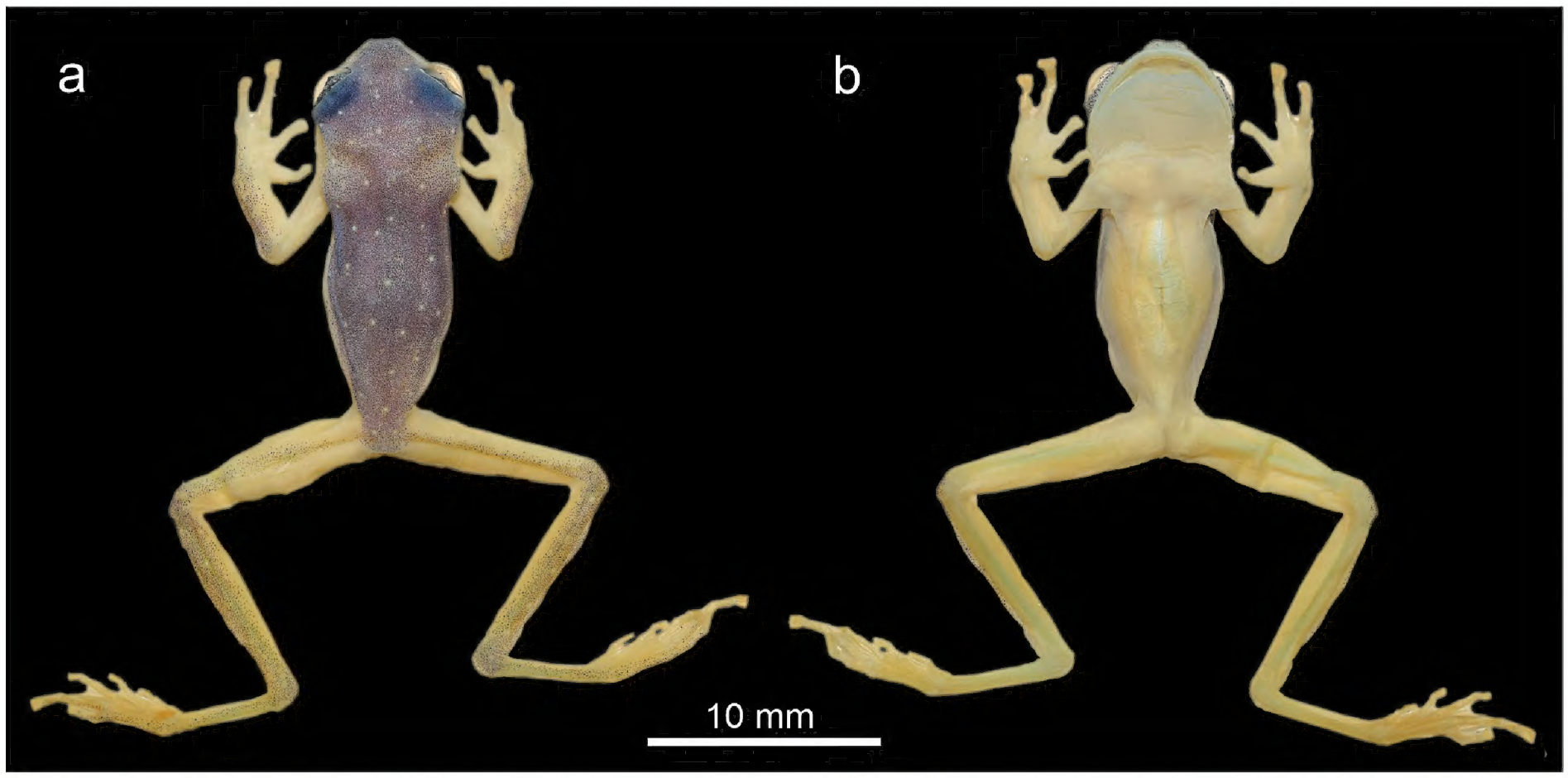

Figure 8. Preserved male holotype of *Chimerella mira* sp. nov. (MUSM 40278, FGZC 6233) in **a** dorsal and **b** ventral views.

the holotype (Fig. 3). Measurements (in mm) of the paratype are as follows: SVL 18.1, HL 5.5, HW 6.7, TD 0.6, IND 1.7, IOD 2.4, ED 2.4, EW 1.3, END 1.4, HaL 5.2, TL 10.7, THL 10.7, FL 7.6.

The male paratype was dissected for inspection of internal organs which appear as follows: liver with two broadly rounded right/left lobes sagittally divided, not forming free flaps, completely covered in iridophores (white), corresponding to state H1 sensu Cisneros-Heredia and McDiarmid (2007). Gall bladder, pericardium, liver and gastrointestinal peritoneum covered in iridophores (white). Kidneys and urinal bladder are tan in colour and thus not covered by iridophores. Testes ovoid and partially covered in a white iridophore reticulum. Distribution of iridophores in visceral peritonea falls into state V5 sensu Cisneros-Heredia and McDiarmid (2007).

Natural history, distribution, and threat status. Both males were collected at the stream bank of the Río Patay Rondos, a medium-sized tributary of the Río Monzon, which itself is part of the Huallaga river system. The habitat consisted of a swampy area, apparently temporarily flooded by the river, with small lentic waterbodies, emerging shrub vegetation and younger trees (Fig. 9). Shortly after dusk, male individuals were sitting on upper surfaces of leaves approximately 0.5 to 2.5 m above the ground while calling during light rainfall. Some fine transverse scratches were visible on the anterior dorsum of the paratype MUSM 40264, arguing for the occurrence of male-male fighting behaviour (e.g., Hutter et al. 2013b). Egg clutches and larvae are unknown. Anuran species found in sympatry were *Boana lanciformis*, *Leptodactylus griseigularis*, and *Adenomera* sp. The glassfrog *Hyalinobatrachium carlesvilai* occurred at nearby sites within a few hundred metres distance. So far, the species is only known from the type locality at an elevation of 798 m, but might be more widespread in the Huallaga River basin at similar elevations.

Figure 9. Type locality and habitat of *Chimerella mira* sp. nov. on the bank of the Río Patay Rondos, a tributary of the Río Monzon: **a** view to the east along the river bed. The yellow arrow indicates the area where both reported specimens were collected; **b** night view of the swampy habitat at the edge of the river showing shrub vegetation from which males were calling.

Because population size, actual range, and thus potential threats are unknown, we propose the IUCN Red List status 'Data Deficient' for *C. mira* (see also Scherz et al. 2019).

Advertisement call. Calls were emitted at somewhat irregular intervals and occurred in 'waves' with several males calling nearly synchronously. The advertisement calls recorded on 5 November 2019 at the type locality (estimated air temperature ca. 25 °C; recording distance approximately 1.5 m) consist of 2 to 3 high-pitched, pulsed notes of short duration (Fig. 10a). Notes exhibit considerable amplitude modulation, with maximum call energy present at the beginning of the note, continuously decreasing towards its end. Pulse structure is rather irregular within notes, with pulses being partly fused and of differing amplitude. As a consequence, the total number of pulses per note is not reliably countable, but in most cases 3 to 4 distinctly separated pulses are evident at the beginning of each note, followed by about 10–12 less distinctly separated pulses. We observed pulse rate within notes to range approximately around 200 pulses/second. Other numerical parameters of 12 analysed calls from 4 individuals are as follows: number of notes per call 2–3 (2.8 ± 0.5); call duration 322–707 ms (552.1 ± 141.8 ms); note duration 42–85 ms (64.6 ± 11.7 ms); inter-note interval within calls 160–239 ms (197.0 ± 26.4 ms); call repetition rate approximately 1.5–1.9 calls/minute; dominant frequency 5543–6135 Hz (5897 ± 148 Hz); prevalent bandwidth 4500–7500 Hz, with weak call energy present up to 21 kHz. Among the notes within a call, dominant frequency is highest in the first note and slightly decreases in subsequent notes. The character of this call would qualify as a 'Trii' call according to the definition of Duarte-Marín et al. (2022).

Comparative call data. The only available call recording of *Chimerella corleone* is that described by Twomey et al. (2014) recorded from a topotypic male in captivity after dislodging it from the female with which it has been in amplexus. These conditions argue for the call representing a mating call, not an advertisement call (J. Delia, pers. comm.) and thus comparison should be regarded with some reservation. However, as mentioned by Twomey et al. (2014), advertisement calls heard in the field were rather similar in character. We re-analysed the available recording of the single call using the methodology described above (for recording equipment used see Twomey et al. 2014). The call (Fig. 10b) has the following numerical parameters: number of notes per call 2; call duration 521 ms; note duration 10 and 15 ms; inter-note interval 493 ms; dominant frequency of the first note 6485 Hz, and 6526 Hz in the second note; prevalent bandwidth difficult to determine due to oversaturated recording level, but call energy is apparently present up to 20 kHz. The character of this call would qualify as a 'Tic' call according to the definition of Duarte-Marín et al. (2022).

Calls of *C. mariaelenae* from Pangayaku Creek (929 m a.s.l.), Provincia Napo, Ecuador, have been described by Guayasamin et al. (2020). The calls (call duration 231–1761 ms) contain 2–10 unpulsed high-pitched notes of very short duration (4–7 ms), repeated at comparatively short intervals. Dominant frequency ranged from 6718–8010 Hz (Guayasamin et al. 2020). Also, Batallas and Brito (2016) described the call of *C. mariaelenae*, from Sangay National Park (1750 m a.s.l.), Provincia Morona Santiago, Ecuador. Their analysis described call parameters quite different from those reported by Guayasamin et al. (2020), with calls always containing 3 notes (call duration 668–808 ms) and much longer note durations of 54–116 ms. The differences among these two call descriptions for calls of *C. mariaelenae* are beyond

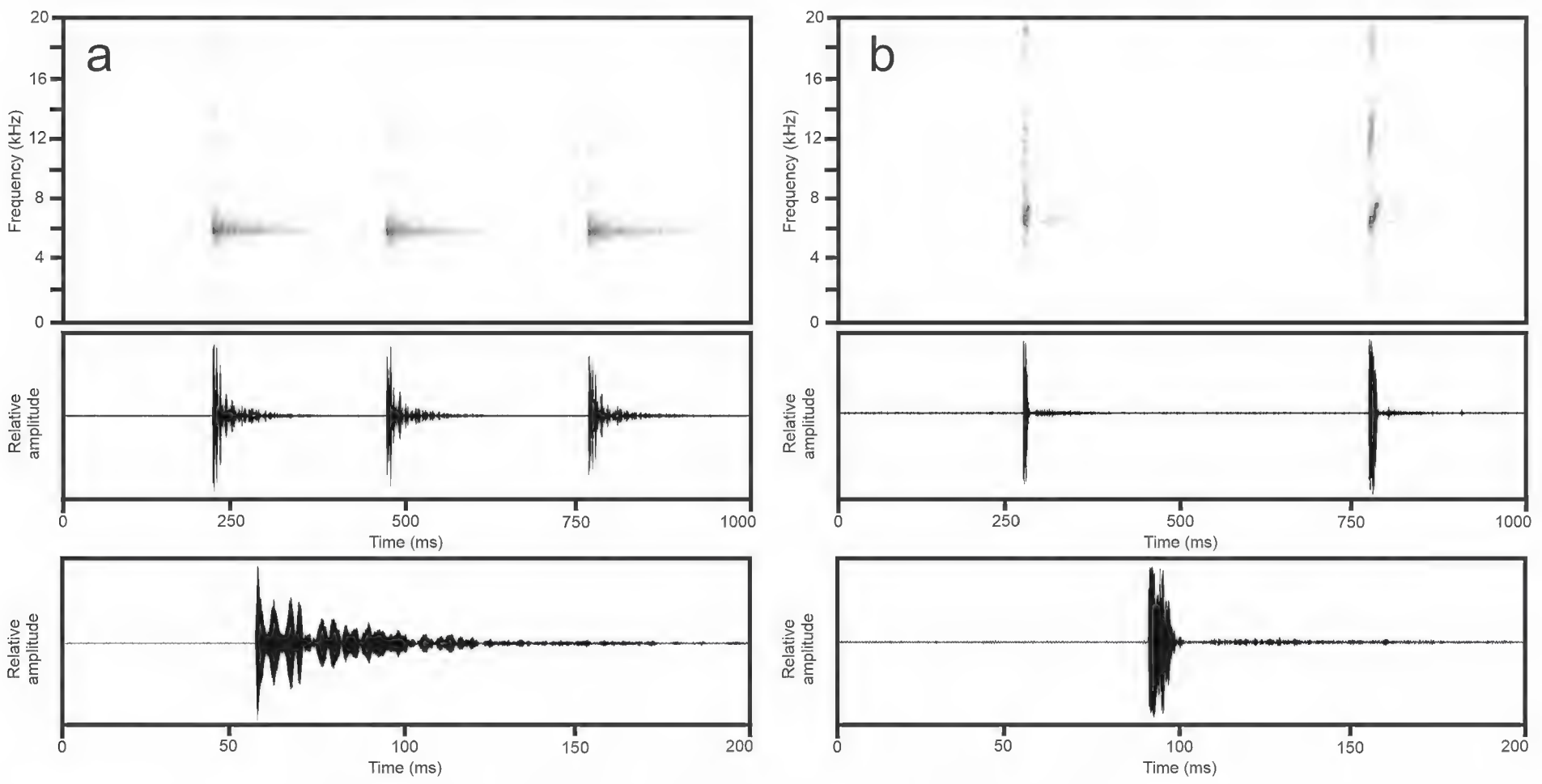

Figure 10. Audiospectrograms and corresponding oscillograms of calls of *Chimerella*: **a** *Chimerella mira* sp. nov. (call voucher MUSM 40264) from west of Tingo Maria, Departamento Huánuco, Peru. Below an expanded oscillogram depicting the first note of the call; **b** *Chimerella corleone* from the type locality, Departamento San Martín, Peru. Below an expanded oscillogram depicting the first note of the call. Both recordings high-pass filtered at 1000 Hz.

those usually considered to represent inter-specific call variation (see Köhler et al. 2017) and would argue for the calls belonging to different species. However, although apparently rare in centrolenids (see Duarte-Marín et al. 2022), the calls described could also refer to two different call types of *C. mariaelenae*. Batallas and Brito (2016) described the males calling in dense choruses containing numerous males, thus territorial and/or aggressive function of the calls recorded could be an explanation. With the data at hand, we are unable to clarify the reason for these call differences described for *C. mariaelenae*, but for our diagnosis above we here relied on the description provided by Guayasamin et al. (2020). However, if considering the calls described by Batallas and Brito (2016) to represent the advertisement call of *C. mariaelenae*, there would be some overlap in numerical parameters with calls of *C. mira*, but the distinct pulsed amplitude structure present in *C. mira* has not been observed in calls described by the mentioned authors.

Discussion

Our study of *Chimerella* glassfrogs in Peru revealed some surprising results. When discovering the specimens west of Tingo Maria, we tentatively identified them as *C. corleone* according to an overall morphological similarity and the fact that the locality is part of the Huallaga River system, which includes the type locality of *C. corleone*, in the Cainarachi valley, further north. On the other hand, specimens collected in northern Peru, occurring at higher elevations in the Departamentos Amazonas and San Martín, are morphologically different when compared to *C. mariaelenae* and *C. corleone* and therefore are believed to represent an undescribed species. Molecular studies, including mitochondrial and nuclear markers, revealed an unexpected picture. The specimens from west of Tingo Maria, at first impression morphologically cryptic to topotypic *C. corleone*, turned out to represent a rather divergent lineage distinguished also by considerable differences in the advertisement call and details of morphology. Although morphologically considerably different, the specimens from higher elevations in Amazonas and San Martín, approximately 160–180 km east of the type locality of *C. corleone* (Fig. 11), were recovered to be part of a clade containing topotypic *C. corleone* and showed only very little genetic differentiation to them in the 16S gene fragment (p-distances 0.2–0.6%), ranging among values typical for intraspecific variation. However, there is apparently no haplotype sharing of these populations with *C. corleone* in the nuclear encoding Rag-1 gene.

As a first consequence of our findings, we here described the clade from west of Tingo Maria as a new species, *Chimerella mira*. Our molecular, morphological, and bioacoustic results provided independent lines of evidence for this population representing a third species in the genus. The genetic divergence between this new species and the two known congeneric species is rather pronounced, being at a similar level of other congeneric species pairs within the Centrolenidae, or even greater, as revealed by cross-checking available GenBank

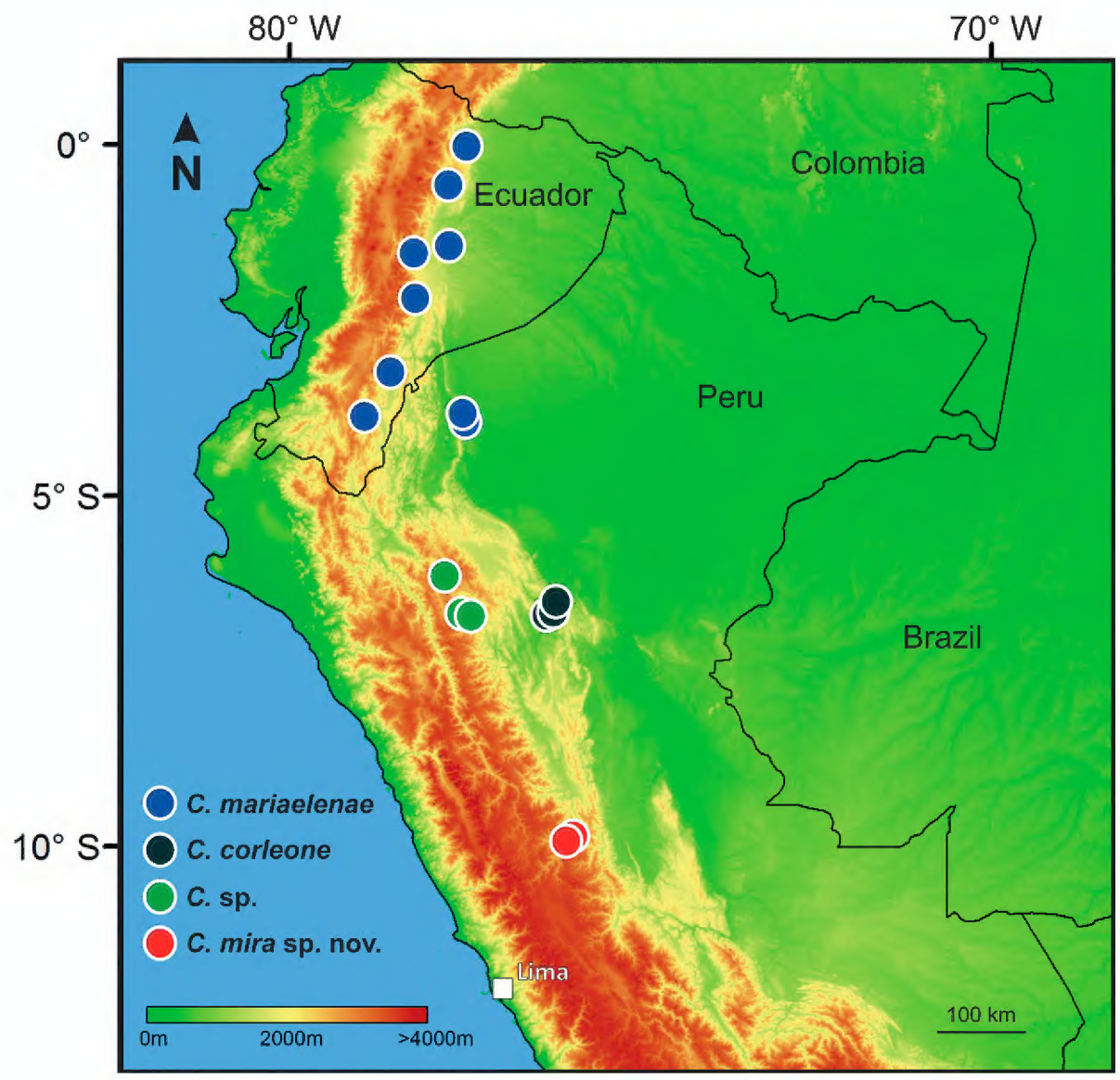

Figure 11. Schematic map of north-western South America indicating the approximate known distribution of *Chimerella* by coloured dots (data for *C. mariaelenae* partly taken from Guayasamin et al. 2020).

sequences. Among the morphological differences found between the three species of *Chimerella*, details in dorsal colour pattern are evident, but most striking are the differences in iris colouration in life, being silvery white with fine dark spotting in *C. mira*, versus silvery grey with dark reticulation in *C. corleone*, and orange to reddish in *C. mariaelenae*. Although these differences may appear negligibly small, iris colouration has proven to be a very reliable diagnostic character in many groups of frogs to distinguish among species (Glaw and Vences 1997), including centrolenids (e.g., Cisneros-Heredia and McDiarmid 2007; Guayasamin et al. 2020). Furthermore, although calls of centrolenid species often share high dominant frequency and short note duration and thus may sound rather similar (Duarte-Marín et al. 2022), the call differences revealed by our call analyses are clearly beyond those considered to represent intra-specific variation (see Köhler et al. 2017). Although the allocation of calls to *C. mariaelenae* includes some uncertainties (see above) and the available call recordings of *C. corleone* may possibly represent a mating call (although similar in character to an advertisement call; see above), calls of *C. mira* differ significantly in qualitative and quantitative traits. This mainly is the presence of multi-pulsed notes versus notes consisting of a single pulse only ('Trii' calls versus 'Tic' calls sensu Duarte-Marín et al. 2022), and the much longer note duration (42–85 ms versus 10–15 ms in *C. corleone* and 4–7 ms in *C. mariaelenae*). In summary, these differences provide multiple lines of evidence for evolutionary lineage divergence and justification for the description of a new species.

Remarkably, the habitat at the type locality of *C. mira* differs considerably from that of *C. corleone*, which has been described as vegetation on vertical rock walls within the spray zone at the edge of waterfalls, where all individuals were exclusively found (Twomey et al. 2014). The association with small, fast flowing streams, providing high air humidity by a certain amount of spray, is a common habitat for many of the stream-breeding centrolenids along the eastern Andean slopes. The swampy habitat of *C. mira* at the edge of a comparatively large river that we report here appears rather different particularly when compared to the habitat of *C. corleone* in being much more exposed, lacking any rock walls and water spray. This would be in agreement with the observations of Rivera and Folt (2018), who found congeneric centrolenids to use different types of habitat. However, as large streams tend to have high water level and strong current during the rainy season, bearing the danger of washing away even larvae with stream-adapted morphology downstream into unsuitable habitat, the habitat of *C. mira* tadpoles remains unknown. It might be hypothesized that either *C. mira* reproduces outside the rainy season (individuals were found at the beginning of the rainy seasons, but no clutches or larvae were observed), or that conditions in the particular habitat, due to the presence of small trees, may provide slow-running lotic conditions at rising water levels suitable for larval development. However, the habitat of *C. mariaelenae* has been described as the edge of small streams and ditches in cloud forest (Cisneros-Heredia and McDiarmid 2007; Guayasamin et al. 2020), and one of us (PJV) observed the species to be abundant in swampy habitats in Sangay National Park, Ecuador, and the Cordillera de Kampankis, northern Peru. *Chimerella* sp. from higher altitudes in Dapartamento Amazonas, Peru, occurred in both types of habitat, namely swampy areas along larger streams as described for *C. mira* and at the edges of small torrential streams. These observations indicate that certain glassfrog species are more flexible with respect to habitat choice when compared to others (see also Rivera and Folt 2018).

Apart from the now three nominal species in the genus *Chimerella*, we are currently unable to clarify the taxonomic status of populations occurring in montane rainforest at around 1800–1900 m a.s.l. in the Departamentos Amazonas and San Martín (Fig. 11), which here were tentatively referred to as *Chimerella* sp. Analyses of mitochondrial markers would argue for conspecifity with *C. corleone*, but on the other hand we found no haplotype sharing in the nuclear marker studied herein (Rag-1). Moreover, the collected specimens exhibit numerous qualitative morphological differences (e.g., colouration, snout shape, dermal fringes) when compared to the three recognized species of *Chimerella*, and undoubtedly these populations would have been described as a separate species without the genetic data available and applying purely morphological species criteria. Because of the striking differences in morphology, we are reluctant to conclude that these frogs represent *C. corleone*, as this would probably constitute a singular case of disproportional polymorphism within a single species of glassfrog. As a consequence, further in-depth studies of these populations are necessary and will be subject of a future contribution. Our findings demonstrate the need for future research to evaluate the taxonomic status of numerous populations of glassfrogs, particularly in Peru, where they remain markedly understudied (see Twomey et al. 2014).

Acknowledgements

We are grateful to the Servicio Nacional Forestal y de Fauna Silvestre (SERFOR) for issuing all necessary scientific permits (RGD 071-2020-MINAGRI-SERFOR-DGGSPFFS, D000067-2021-MINAGRI-SERFOR-DGGSPFFS). We are deeply indebted to Jesse Delia and Evan Twomey for sharing their knowledge, providing call recordings and photographs of *C. corleone* for comparison. We thank Joke Evenblij and Carla Hübner for their help with laboratory work. Beatriz Alvarez Dorda and Santiago Castroviejo-Fisher kindly helped to provide DNA extractions from the MNCN collection. We are furthermore grateful to Diego F. Cisneros-Heredia, Brian Folt, Evan Twomey, and an anonymous reviewer for their time and valuable comments on the manuscript.

References

Batallas D, Brito J (2016) Análisis bioacústico de las vocalizaciones de seis especies de anuros de la laguna Cormorán, complejo lacustre de Sardinayacu, Parque Nacional Sangay, Ecuador. Revista Mexicana de Biodiversidad 87: 1292–1300. https://doi.org/10.1016/j.rmb.2016.10.005

Bossuyt F, Milinkovitch MC (2000) Convergent adaptive radiations in Madagascan and Asian ranid frogs reveal covariation between larval and adult traits. Proceedings of the National Academy of Sciences of the United States of America 97: 6585–6590. https://doi.org/10.1073/pnas.97.12.6585

Castillo-Urbina E, Glaw F, Aguilar-Puntriano C, Vences M, Köhler J (2021) Genetic and morphological evidence reveal another new toad of the *Rhinella festae* species group (Anura: Bufonidae) from the Cordillera Azul in central Peru. Salamandra 57: 181–195. https://doi.org/10.5281/zenodo.4767016

Catenazzi A, Venegas PJ (2012) Anfibios y reptiles/Amphibians and reptiles. In: Pitman N, Ruelas Inzunza E, Alvira Reyes D, Vriesendorp C, Moskovitz D, del Campo A, Wachter T, Stotz DF, Noningo S, Tuesta E, Smith RC (Eds) Perú: Cerros de Kampankis. Rapid Biological and Social Inventories Report 24: 106–117. [Spanish] [260–271 [English]]

Chiari Y, Vences M, Vieites DR, Rabemananjara F, Bora P, Ramilijaona Ravoahangimalala O, Meyer A (2004) New evidence for parallel evolution of colour patterns in Malagasy poison frogs (*Mantella*). Molecular Ecology 13: 3763–3774. https://doi.org/10.1111/j.1365-294X.2004.02367.x

Cisneros-Heredia DF (2009) Amphibia, Anura, Centrolenidae, *Chimerella mariaelenae* (Cisneros-Heredia and McDiarmid, 2006), *Rulyrana flavopunctata* (Lynch and Duellman, 1973), *Teratohyla pulverata* (Peters, 1873), and *Teratohyla spinosa* (Taylor, 1949): Historical records, distribution extension and new provincial record in Ecuador. Check List 5: 912–916. https://doi.org/10.15560/5.4.912

Cisneros-Heredia DF, Guayasamin JM (2007) Amphibia, Anura, Centrolenidae, *Centrolene mariaelenae*: distribution extension, Ecuador. Check List 2: 93–95. https://doi.org/10.15560/2.3.93

Cisneros-Heredia DF, McDiarmid RW (2006) A new species of the genus *Centrolene* (Amphibia: Anura: Centrolenidae) from Ecuador with comments on the taxonomy and biogeography of glassfrogs. Zootaxa 1244: 1–32. https://doi.org/10.11646/zootaxa.1244.1.1

Cisneros-Heredia DF, McDiarmid RW (2007) Revision of the characters of Centrolenidae (Amphibia: Anura: Athesphatanura), with comments on its taxonomy and the description of new taxa of glassfrogs. Zootaxa 1572: 1–82. https://doi.org/10.11646/zootaxa.1572.1.1

Delia J, Bravo-Valencia L, Warkentin KM (2017) Patterns of parental care in Neotropical glassfrogs: fieldwork alters hypotheses of sex-role evolution. Journal of Evolutionary Biology 30(5): 898–914. https://doi.org/10.1111/jeb.13059

Duarte-Marín S, Rada M, Rivera-Correa M, Caorsi V, Barona E, González-Duran G, Vargas-Salinas F (2022) Tic, Tii and Trii calls: Advertisement call descriptions for eight glass frogs from Colombia and analysis of the structure of auditory signals in Centrolenidae. Bioacoustics 32(2): 143–180. https://doi.org/10.1080/09524622.2022.2077833

Frost DR (2023) Amphibian Species of the World: an Online Reference. Version 6.1 [accessed 4 May 2023] Electronic Database accessible at American Museum of Natural History, New York. https://amphibiansoftheworld.amnh.org/index.php.

Glaw F, Vences M (1997) Anuran eye colouration: definitions, variation, taxonomic implications and possible functions. In: Böhme W, Bischoff W, Ziegler T (Eds) Herpetologia Bonnensis. SEH Proceedings, Bonn, 125–138.

Guayasamin JM, Castroviejo-Fisher S, Trueb L, Ayarzagüena J, Rada M, Vilà C (2008) Phylogenetic relationships of glassfrogs (Centrolenidae) based on mitochondrial and nuclear genes. Molecular Phylogenetics and Evolution 48: 574–595. https://doi.org/10.1016/j.ympev.2008.04.012

Guayasamin JM, Castroviejo-Fisher S, Trueb L, Ayarzagüena J, Rada M, Vilà C (2009) Phylogenetic systematics of glassfrogs (Amphibia: Centrolenidae) and their sister taxon *Allophryne ruthveni*. Zootaxa 2100: 1–97. https://doi.org/10.11646/zootaxa.2100.1.1

Guayasamin JM, Cisneros-Heredia DF, McDiarmid RW, Peña O, Hutter CR (2020) Glassfrogs of Ecuador: diversity, evolution and conservation. Diversity 12(6): e222. https://doi.org/10.3390/d12060222

Hrbek T, Larson A (1999) The evolution of diapause in the killifish family Rivulidae (Atherinomorpha, Cyprinodontiformes): a molecular phylogenetic and biogeographic perspective. Evolution 53: 1200–1216. https://doi.org/10.2307/2640823

Hutter CR, Esobar-Lasso S, Rojas-Morales JA, Gutiérrez-Cárdenas PDA, Imba H, Guayasamin JM (2013b) The territoriality, vocalizations and aggressive interactions of the red-spotted glassfrog, *Nymphargus grandisonae* Cochran and Goin, 1970 (Anura: Centrolenidae). Journal of Natural History 47: 3011–3032. https://doi.org/10.1080/00222933.2013.792961

Hutter CR, Guayasamin JM, Wiens JJ (2013a) Explaining Andean megadiversity: the evolutionary and ecological causes of glassfrog elevational richness patterns. Ecology Letters 16(9): 1135–1144. https://doi.org/10.1111/ele.12148

Kalyaanamoorthy S, Minh BQ, Wong TKF, von Haeseler A, Jermiin LS (2017) ModelFinder: Fast model selection for accurate phylogenetic estimates. Nature Methods 14: 587–589. https://doi.org/10.1038/nmeth.4285

Katoh K, Standley DM (2013) MAFFT multiple sequence alignment software version 7: improvements in performance and usability. Molecular Biology and Evolution 30: 772–780. https://doi.org/10.1093/molbev/mst010

Kocher TD, Thomas WK, Meyer A, Edwards SV, Pääbo S, Villablanca FX, Wilson AC (1989) Dynamics of mitochondrial DNA evolution in animals: Amplification and sequencing with conserved primers. Proceedings of the National Academy of Sciences of the United States of America 86: 6196–6200. https://doi.org/10.1073/pnas.86.16.6196

Köhler J, Castillo-Urbina E, Aguilar-Puntriano C, Vences M, Glaw F (2022) Rediscovery, redescription and identity of *Pristimantis nebulosus* (Henle, 1992), and description of a new terrestrial-breeding frog from montane rainforests of central Peru (Anura, Strabomantidae). Zoosystematics and Evolution 98: 213–232. https://doi.org/10.3897/zse.98.84963

Köhler J, Jansen M, Rodríguez A, Kok PJR, Toledo LF, Emmrich M, Glaw F, Haddad CFB, Rödel M-O, Vences M (2017) The use of bioacoustics in anuran taxonomy: theory, terminology, methods and recommendations for best practice. Zootaxa 4251: 1–124. https://doi.org/10.11646/zootaxa.4251.1.1

Kumar S, Stecher G, Tamura K (2016) MEGA7: Molecular evolutionary genetics analysis version 7.0 for bigger datasets. Molecular Biology and Evolution 33: 1870–1874. https://doi.org/10.1093/molbev/msw054

Librado P, Rozas J (2009) DnaSP. Version 5. A software for comprehensive analysis of DNA polymorphism data. Bioinformatics 25: 1451–1452. https://doi.org/10.1093/bioinformatics/btp187

Martin AP (1999) Substitution rates of organelle and nuclear genes in sharks: implicating metabolic rate (again). Molecular Biology and Evolution 16: 996–1002. https://doi.org/10.1093/oxfordjournals.molbev.a026189

McDiarmid RW (1994) Preparing amphibians as scientific specimens. In: Heyer WR, Donnelly MA, McDiarmid RW, Hayek L-AC, Foster MS (Eds) Measuring and Monitoring Biological Diversity. Standard Methods for Amphibians. Smithsonian Institution Press, Washington, 289–296.

Nguyen LT, Schmidt HA, von Haeseler A, Minh BQ (2015) IQ-TREE: a fast and effective stochastic algorithm for estimating maximum-likelihood phylogenies. Molecular Biology and Evolution 32: 268–274. https://doi.org/10.1093/molbev/msu300

Palumbi SR, Martin A, Romano S, McMillan WO, Stice L, Grabowski G (1991) The Simple Fool's Guide to PCR, Version 2.0. Privately published, University of Hawaii.

Puillandre N, Brouillet S, Achaz G (2021) ASAP: assemble species by automatic partitioning. Molecular Ecology Resources 21: 609–620. https://doi.org/10.1111/1755-0998.13281

Rivera N, Folt B (2018) Community assembly of glass frogs (Centrolenidae) in a Neotropical wet forest: a test of the river zonation hypothesis. Journal of Tropical Ecology 34: 108–120. https://doi.org/10.1017/S0266467418000068

Salzburger W, Ewing GB, von Haeseler A (2011) The performance of phylogenetic algorithms in estimating haplotype genealogies with migration. Molecular Ecology 20: 1952–1963. https://doi.org/10.1111/j.1365-294X.2011.05066.x

Scherz MD, Glaw F, Hutter CR, Bletz MC, Rakotoarison A, Köhler J, Vences M (2019) Species complexes and the importance of Data Deficient classification in Red List assessments: The case of *Hylobatrachus* frogs. PLoS ONE 14(8): e0219437. https://doi.org/10.1371/journal.pone.0219437

Stephens M, Smith NJ, Donnelly P (2001) A new statistical method for haplotype reconstruction from population data. American Journal of Human Genetics 68: 978–989. https://doi.org/10.1086/319501

Taboada C, Delia J, Chen M, Ma C, Peng X, Zhu X, Jiang L, Vu T, Zhou Q, Yao J, O'Connell L, Johnsen S (2022) Glassfrogs conceal blood in their liver to maintain transparency. Science 378(6626): 1315–1320. https://doi.org/10.1126/science.abl6620

Terán-Valdez A, Guayasamin JM (2014) The tadpole of the glassfrog *Chimerella mariaelenae* (Anura: Centrolenidae). CienciAmérica 3: 17–22.

Twomey E, Delia J, Castroviejo-Fisher S (2014) A review of northern Peruvian glassfrogs (Centrolenidae), with the description of four new remarkable species. Zootaxa 3851: 1–87. https://doi.org/10.11646/zootaxa.3851.1

Vences M, Kosuch J, Glaw F, Böhme W, Veith M (2003) Molecular phylogeny of hyperoliid treefrogs: biogeographic origin of Malagasy and Seychellean taxa and re-analysis of familial paraphyly. Journal of Zoological Systematics and Evolutionary Research 41: 205–215. https://doi.org/10.1046/j.1439-0469.2003.00205.x

Vences M, Miralles A, Brouillet S, Ducasse J, Fedosov A, Kharchev V, Kostadinov I, Kumari S, Patmanidis S, Scherz MD, Puillandre N, Renner SS (2021) iTaxoTools 0.1: Kickstarting a specimen-based software toolkit for taxonomists. Megataxa 6: 77–92. https://doi.org/10.11646/megataxa.6.2.1

Vences M, Patmanidis S, Kharchev V, Renner SS (2022) Concatenator, a user-friendly program to concatenate DNA sequences, implementing graphical user interfaces for MAFFT and FastTree. Bioinformatics Advances 2: vbac050. https://doi.org/10.1093/bioadv/vbac050